From At-Sensor Observation to At-Surface Reflectance – Calibration Steps for Earth Observation Hyperspectral Sensors

H. Peter White[*†], K. Shahid Khurshid[†], Robert Hitchcock[‡], Robert Neville[†], Lixin Sun[§], Catherine M. Champagne[#], and Karl Staenz[†]
[†]Canada Centre for Remote Sensing, Natural Resources Canada, 588 Booth St., Ottawa, Ontario, Canada, K1A 0Y7
[‡]Prologic Systems Limited, Ottawa, Ontario, Canada, K1P 5E7
[§]Dendron Resource Surveys Inc., Ottawa, Ontario, Canada, K1Z 5L9
[#]Mir Télédédection Inc., Longueuil, Québec, Canada, J4K 1A3
[*]Corresponding Author Email : PWhite@NRCan.gc.ca

***Abstract* – With the continued development of space borne hyperspectral sensors (CSA HERO, ESA CHRIS-on-PROBA, ESA SPECTRA, NASA SpectraSat) to follow the EO-1 Hyperion sensor, high spectral and spatial Earth observation data will become more readily available to the research and user communities. With this improvement in spectral and spatial resolution comes the need to have more rigorous image pre-processing. Spectral and spatial registration and radiometric response need to be characterized and applied more frequently, possibly on a scene by scene basis depending on the stability of the sensor. This requires a system that can evaluate a dataset and determine these parameters efficiently and independently.**

A pre-processing procedure to transform at-sensor signals to at-surface reflectance for Earth Observation hyperspectral imagery has been developed at the Canada Centre for Remote Sensing / Natural Resources Canada (CCRS/NRCan). This process examines an image cube for bad pixels (stripes) and noise levels, determines spectral (smile effect) and spatial (keystone) registration per pixel, as well as evaluating the image cube for optimal signal gain and offset, and applies the relevant corrections. Where applicable, a scene-based (vicarious) calibration procedure can also be applied.

I. Introduction

A procedure has been developed to measure and correct for effects of detector artefacts associated with using imaging spectrometers for hyperspectral remote sensing of the Earth's surface. These artefacts include such things as spectral smile (or frown), keystone, detector alignment (for systems using multiple detectors), sensor gain and offset, and sensor noise.

With an imaging spectrometer utilizing a two-dimensional detector array, the spectrum is dispersed in one dimension (the columns) and the spatial field is oriented orthogonal to this (the rows or lines). In ideal conditions, this type of imaging provides two-dimensional (spectral-spatial) frames of data where all the information in a given column refers to a unique spot on the ground, and all the information in a given row represents a characterized single band centre wavelength and band width. Spectral line curvature and geometric distortions caused by the optical components of the sensor can result in spectral and spatial mis-registration of the pixels.

When the detector is well characterized, gains and offsets required to convert this information to at-sensor radiance are applied to derive the requested hyperspectral imagery. For several sensors, multiple detectors are used to provide data for several spectral regions (commonly referred to as visible, near infrared, and short-wave infrared). Such systems require additional processing steps of aligning the detectors.

In the following sections, a brief description of the methods used to detect these artefacts and apply the appropriate corrections is presented. Detailed discussions of specific individual detection methods are referenced where appropriate. Trails of these stages in processing from at-sensor to at-surface reflectance have been tested on a variety of hyperspectral imagery sources, such as the Airborne Visible/Infrared Imaging Spectrometer (AVIRIS), the Compact Airborne Spectrographic Imager (*casi*), SWIR (Short Wave Infra-Red) Full Spectrum Imager (SFSI) and EO-1 Hyperion and have been published separately. This procedure has been developed using the Natural Resources Canada / Canada Centre for Remote Sensing (CCRS) Imaging Spectrometer Data Analysis System (ISDAS) [1].

II. Processing Steps

When hyperspectral image data has been received, it will often come with gain and offset information applied to provide at-sensor radiance imagery (a scale factor may also be applied at this stage). Mean band centre wavelengths and bandwidths are also provided This level of data is used as the start information in the processing chain (shown in Fig 1.).

A. Detector Alignment

When multiple detectors are used to provide a wider spectral or spatial coverage, they can become mis-aligned or purposely positioned within the instrument off-set from each

other. For example, the Hyperion SWIR detector is such that columns 129-256 must be shifted up one row to align with columns 1-128 [2]. The SWIR detector must then be aligned to the VNIR detector.

Once a basic spatial shift is performed to align pixels within each detector, the detectors are compared to detect spatial and angular shifts required to align one detector to another. The Angular-Shift correction compares two image planes, one from each detector, and determines the sub-pixel shift and angular rotation required to align the detectors.

B. Destriping

Stripes (columns of data of poor quality within an image plane) can occur due to systematic noise such as detector non-linearities, temperature effects [3] or functional failure of a single detector element during image acquisition. For cases of a dead pixel, the stripe will contain no information and the pixel is replaced using a linear interpolation between the two closest valid pixels.

Automatic destriping of other pixels is performed using both spatial and spectral information of adjacent pixels. Spectral information is used to determine a "natural variation"

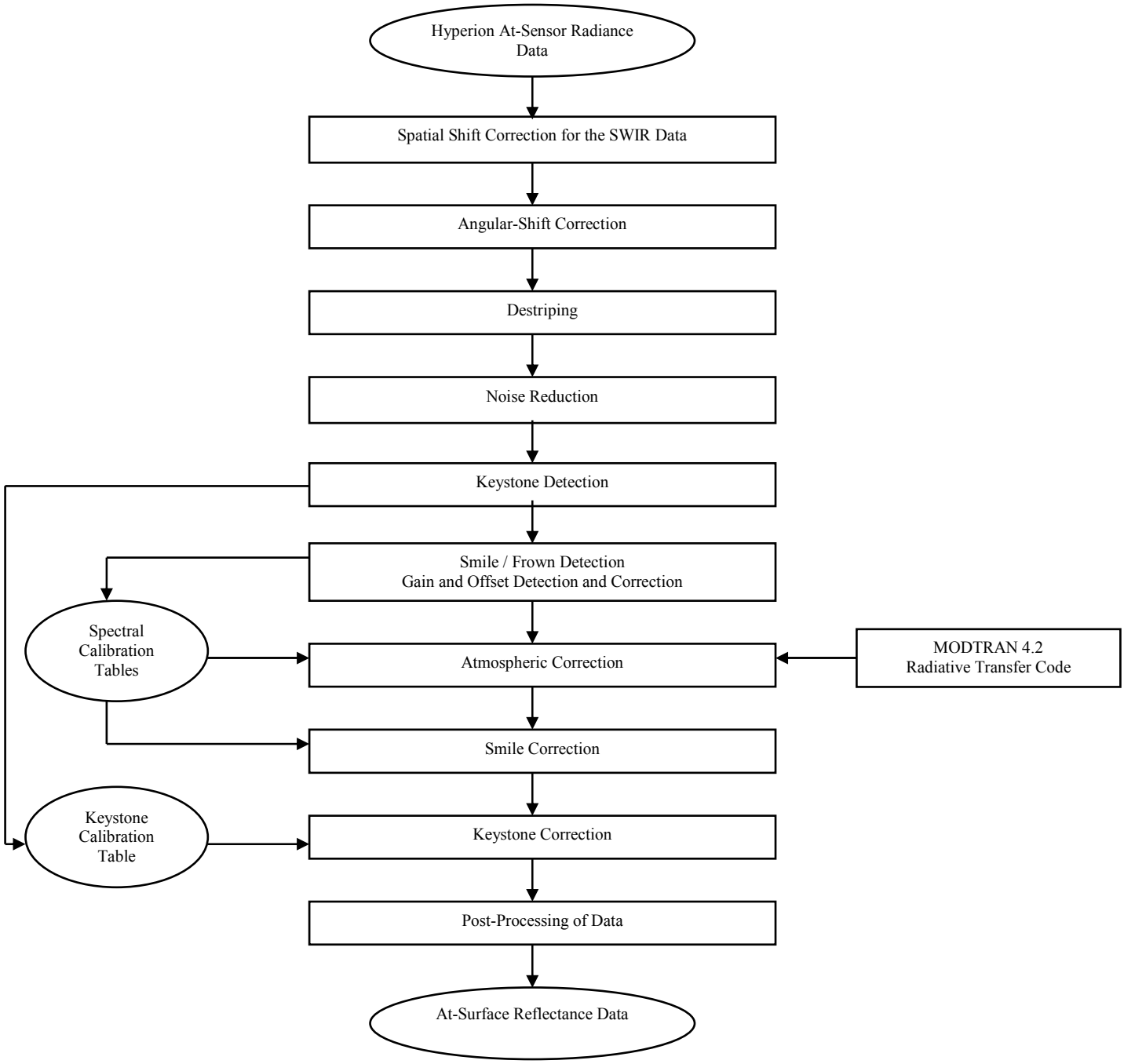

Figure 1: Hyperspectral data preprocessing steps for retrieval of at-surface reflectance from at-sensor radiance.

for each pixel. The "natural variation" is determined by first averaging radiance values per band (average pixel value per image plane), then evaluating the differences of neighbouring average pixels over a set of neighbouring bands. This information is then applied to destripe the column if the difference between the pixel average and the surrounding pixel averages is significantly different than the "natural variation". This method is done iteratively to identify average pixel values which are significantly higher or lower than the surrounding average pixels across a band set until all average pixels are within the "natural variation" [4].

C. Noise Reduction

Noise reduction is an important step towards improving the quality of the remotely sensed hyperspectral data, especially when the signal level is low or the detector performance is poor.

To reduce the impact of noise on the data, an "average smoothing" procedure has been developed. A modelled noise cube ($n_{i,j,k}$) is first produced given the initial pixel radiance values per image plane, $v_{i,j,k}$, and the Digital Number (DN) to radiance gain, $g_{j,k}$, using (1):

$$n_{i,j,k} = \sqrt{\left(N_f \cdot g_{j,k}\right)^2 + \frac{v_{i,j,k} \cdot g_{j,k}}{c}} \qquad (1)$$

where N_f and c are the floor noise and the charge conversion factor of the detector respectively.

Here, a limited number of columns around a pixel are examined for spectra of similar shape and magnitude (a limited number of columns are used to reduce the effect of spectral smile and atmospheric contributions). The noise cube is used to define a noise boundary, allowing the identification pixels which are spectrally similar (which have spectral variations within the noise boundary of the pixel being examined). An average spectrum is then determined and is used to replace the original for that pixel. Each pixel is examined individually. Once complete, a spectral noise cube is produced to demonstrate the level of noise determined for each pixel [5].

D. Keystone Detection

The term "keystone" is used by the hyperspectral remote sensing community when inter-band spatial mis-registration occurs in imaging spectrometers. This results in a variation of spatial scale in the across-track direction as a function of spectral band (or image plane).

Keystone distortions are evaluated for each detector of the hyperspectral sensor separately. Prominent features are first identified in the image using edge detection. The spatial location of these features are then determined per image plane relative to a reference plane. Sub-pixel shifts are calculated by using a sliding sub-window over each feature to determine a correlation coefficient. Shift values per band for each feature are then fitted to a quadratic polynomial to provide a keystone calibration matrix containing the per pixel shift as a function of image band for each detector. The matrix is applied to the imagery after other artefacts have been evaluated. This technique has been demonstrated to identify keystone shifts of less than 0.01 pixels [6].

E. Spectral Line Curvature and Radiance Gain/Offset Determination

Many imaging spectrometers exhibit spectral line curvature (spectral smile or frown). Due to the curvature of the focal plane of each spectral band, each image plane has an across-track band centre and bandwidth shift. Thus each column in a hyperspectral image can have unique spectral band centres and bandwidths. Atmospheric correction of this imagery will result in spikes of varying magnitude across-track in the derived at-surface reflectance spectra near atmospheric absorption features [7].

A technique has been developed at CCRS which uses these atmospheric absorption features to determine and later adjust the across-track band centres and bandwidths. Using the MODTRAN4v2 radiative transfer code, at-sensor radiance to at-surface reflectance calibration look-up-tables (LUTs) are created for a range of band centres and bandwidths (the range for each is centred on the mean band centre and bandwidth values provided with the original imagery) in the region of the absorption features (as outlined in Table 1). Using these LUTs, modelled at-sensor radiances are compared to the original data for different atmospheric absorption features. The band centre / bandwidth combination which best correlates to the measured at-sensor radiances is determined through an iterative procedure and a spectral line curvature matrix identifying the across-track band centre and bandwidth calibrations is saved. This may result in a derived at-sensor radiance (v) which is slightly different to the original value (v^o). If this is the case, then slight adjustments are also required to the reported gains ($g_{j,k} \rightarrow g_{j,k} \times \Delta g_{j,k}$) and offsets ($o_{j,k} \rightarrow o_{j,k} + \Delta o_{j,k}$).

Once band centres and bandwidths are determined across the image, bright (v_b) and dark (v_d) pixels are identified for each column at each band near the atmospheric features. If the original gains and offsets which transform sensor DN to at-sensor radiance are provided, then they are applied to the data

TABLE 1
ATMOSPHERIC ABSORPTION FEATURES SELECTED FOR SMILE DETECTION. ABSORPTION MINIMUMS ARE ADAPTED FROM SCHLAPFER (1998) [8].

Atmospheric Constituent	Wavelength Range (nm)	Absorption Minimum (nm)
Ozone (O_3)	457 538	574
Oxygen (O_2)	732 782	687
Water (H_2O)	782 854	823
Water (H_2O)	912 1003	942
Water (H_2O)	1013 1235	1134
Oxygen (O_2)	1235 1295	1268
Carbon Dioxide (CO_2)	1548 1638	1601
Carbon Dioxide (CO_2)	2022 2113	2055
Methane (CH_4)	2244 2355	2276, 2317

and the bright and dark pixels are evaluated to determine if additional adjustments are required [8]. Adjustments to the gains and offsets are derived using (2).

$$\Delta g_{j,k} = \left(\nu_{b,j,k} - \nu_{d,j,k}\right) \Big/ \left(\nu^{o}_{b,j,k} - \nu^{o}_{d,j,k}\right)$$
$$\Delta o_{j,k} = \frac{\left(\nu_{d,j,k} \times \nu^{o}_{b,j,k} - \nu_{b,j,k} \times \nu^{o}_{d,j,k}\right)}{g_{j,k} \times \left(\nu_{b,j,k} - \nu_{d,j,k}\right)} \qquad (2)$$

F. Post-Processing of Data

Once pre-processing is complete, the reflectance spectra in high noise (low signal) regions are examined for quality purposes. If warranted, a post-processing step is included. This involves the calculation of correction gains and offsets using a spectrally flat target pixel approach [10]. This technique assumes that a number of pixels (selected automatically) exist which are spectrally flat (feature-less) in the region of interest. Linear fits are determined for these feature-less spectra, which is used to determine the correction gains and offsets which are then applied to the whole image in these high noise (low signal) bands.

III. Impact

The magnitude of the influence of each artefact discussed above is different for different sensors. Together, they can result in significant apparent noise in the at-sensor radiance and subsequent derived at-surface reflectance. The impacts of each step has been discussed for various sensors in other publications and the readers are encouraged to review them.

One randomly selected pixel (vegetation) is provided in Fig. 2 to demonstrate the result of applying the above processing steps to a Hyperion image. The pixel was extracted from a processed image which was acquired of an agricultural area in Indian Head, Saskatchewan in June, 2002. Note the lack of sharp peaks near the atmospheric water absorption lines and the reduction of noise after using the above processing steps.

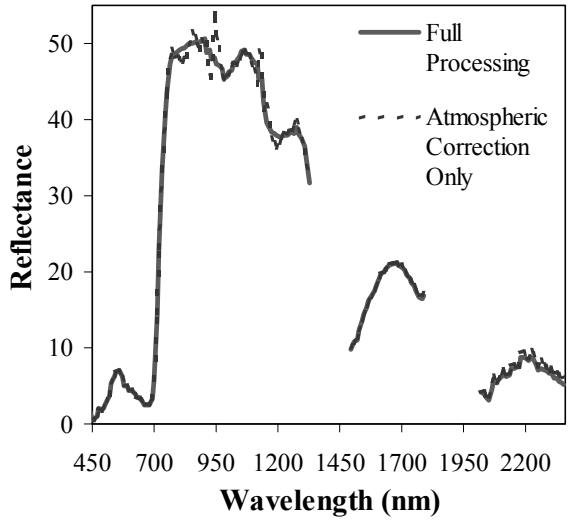

Figure 2 : Comparison of a single pixel reflectance spectra for vegetation using (solid) and not using (dashed) the processing chain.

IV. Summary

A methodology has been presented here which permits the derivation of at-surface reflectance from at-sensor radiance for hyperspectral sensors which also examines the imagery data for potential artefacts. Impacts of poor pixel response and spatial and spectral mis-registration are evaluated as part of the pre-processing process, thus providing a tool for determining at-surface reflectance for a variety of hyperspectral sensors, without having to know specific, and sometimes time dependant, detector element calibrations.

References

[1] K. Staenz, T. Szeredi and J. Schwarz, "ISDAS – A System for Processing/Analysing Hyperspectral Data", *Can. J. Rem. Sens.* **24**(2):99-113, 1998.

[2] J.S. Pearlman, P.S. Barry, C.C. Segal, J. Shepanski, D. Beiso and S.L. Carman, "Hyperion, a Space-Based Imaging Spectrometer", *IEEE Trans. Geosci. Rem. Sens.* **41**(6): 1160-1173, 2003.

[3] F.A. Kruse, J.W. Boardman and J.F. Huntington, "Comparison of Airborne Hyperspectral Data EO-1 Hyperion for Mineral Mapping", *IEEE Trans. Geosci. Rem. Sens.* **41**(6): 1388-1400, 2003.

[4] S.K. Khurshid, *Estimation and Mapping of Wheat Crop Chlorophyll Content Using Hyperion Hyperspectral Data*, M.Sc. Thesis, Dept. Geography, University of Ottawa, 2004.

[5] L. Sun, "Average Smoothing Module – Help File", ISDAS Release June 2004.

[6] R.A. Neville, L. Sun and K. Staenz, "Detection of Keystone in Imaging Spectrometer Data", *Algorithms and Technologies for Multispectral, Hyperspectral, and Ultraspectral Imagery IX*, S.S. Shen, P.E. Lewis, editors, **5093**: 144-154, SPIE, Bellingham, 2003.

[7] R.A. Neville, L. Sun and K. Staenz, "Detection of Spectral Line Curvature in Imaging Spectrometer Data", *Algorithms and Technologies for Multispectral, Hyperspectral, and Ultraspectral Imagery IX*, S.S. Shen, P.E. Lewis, editors, **5093**: 144-154, SPIE, Bellingham, 2003.

[8] D. Schlapfer, C.B. Christoph, J. Keller and K.I. Itten, "Atmospheric Precorrected Differential Absoprtion Technique to Retrieve Columnar Water Vapor", *Rem Sens, Environ.* **65**:353-366, 1998.

[9] L. Sun, "Smile Detector Module – Help File", ISDAS Release June 2004.

[10] K. Steanz, R.A. Neville, J. levesque, T. Szeredi, V. Singhroy, G.A. Borstad and P. Hauff , "Evaluation of CASI and SFSI Hyperspectral Data for Environmental and Geological Applications – Two Case Studies", *Can. J. Rem. Sens.* **25**(3):311-322, 1999.